

adhesion of the electrode to the substrate and substrate morphology. In order to improve electrical properties of the front electrode, various fabrication techniques are being analyzed, consisting in different imprint techniques and its final connection with the substrate surface. On one hand, basing on available literature studies [1-15] and author's own research [1-5] it can be stated that most popular and currently used method is the conventional screen printing method combined with co-firing in the furnace for front electrode production. On the other hand, there are few examples in literature concerning fabrication of front metallization by selective laser sintering [16-17], they induced the authors to take presented approach.

The name "artificial neural networks" describes the hardware or software simulators, which are realizing semi parallel data processing. They are built from many mutually joined neurons and they imitate the work of biological brain structures [23]. McCulloch and Pitts worked out the scheme of the neuron in 1943 and it was created as a building imitation of the biological nervous cell [21,22]. Equation 1 describes the mathematical model, where m is a number of input signals of a single neuron.

$$y = \phi \left(\sum_{i=1}^m w_i x_i \right) \quad (1)$$

The fundamental difference between artificial neural networks is the ability to generalize the knowledge for new given data, which were unknown earlier and which were not presented during the training process. In distinction from expert systems, which require the permanent access to whole assembly of knowledge on the subject about which they will decide, artificial neural networks requiring only single access to this data set in the process of training. Neural networks reveal the tolerance on discontinuities, accidental disorders or lacks of data in the descriptive vectors. This allows application of artificial neural networks for problems, that cannot be solved by any other algorithm or their implementation will not give any satisfactory results [20,22,23].

2. Experimental procedure

The investigations were done on the monocrystalline silicon wafers of p type doped with boron and area 50x50cm², as well resistivity $\sim 1 \div 3 \Omega \cdot \text{cm}$. The wafers with thickness $\sim 330 \mu\text{m}$ were processed with the SLS method, whereas those of about $\sim 230 \mu\text{m}$ were processed with the SP method and co-fired in the furnace. The fabrication sequence of solar cells is presented in Figure 1. Table 1 presents selection of elements in contact layer of solar cell. Two silver powders were applied during investigations of the following granulations: 40 μm and 40 nm in order to both the optimal granulation and powder. Selection of chemical composition of front contact was carried out experimentally and mixtures were prepared using the mechanical mixer.

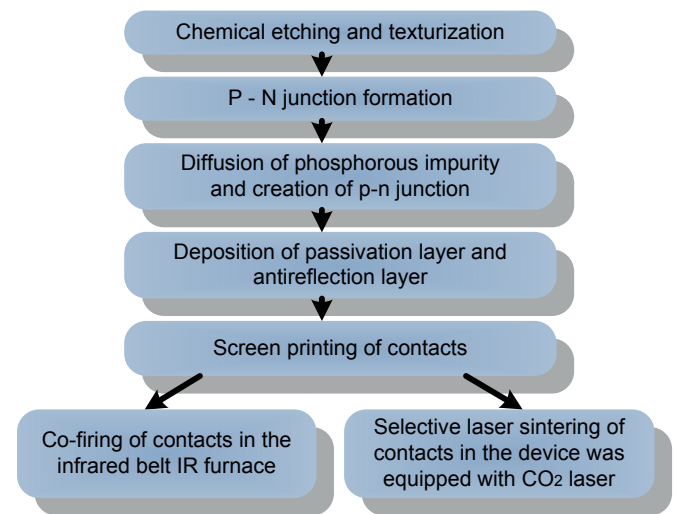


Fig. 1. Scheme of the technological process of solar cells manufacturing

Two special test electrode systems were prepared by screen printing method in order to demonstrate usefulness of silver pastes and to evaluate the contact resistance of the silver electrode-silicon junction:

- I. sizes of front paths were: 2 x 10 mm (wide x length),

TABLE 1

The paste properties

Paste symbol	Mass concentration of elements, %			Surface morphology of the solar cell
	Basic powder	Organic carrier	Ceramic glaze	
Selective laser sintering				
A	83	15	2	1, 2, 3, 4
B	88.40	9.60	2	1, 2, 3, 4
Co – firing in the furnace				
C	88.40	11.60	-	1, 2
D	85	15	-	3, 4
E	60.60	39.40	-	1, 2
F	83.33	16.67	-	3, 4
PV145*	-	-	-	1, 2, 3, 4

Where: 1. non-textured with deposited TiO_x coating, 2. non-textured without deposited TiO_x coating, 3. textured with deposited TiO_x coating, 4. textured without deposited TiO_x coating, * commercial paste manufactured by Du Pont

distances between them were: 20 mm, 10 mm, 5 mm, 2.5 mm,

- II. sizes of front paths were: 5 x 10 mm (wide x length), distances between them were: 1 mm, 2 mm, 4 mm, 8 mm.

The most beneficial conditions of laser micro-treatment were selected based on both the initial tests and metallographic observations. Table 2 presents the selected laser micro-treatment conditions for the test electrodes system I, II. The investigations were performed using the Eosint M 250 Xtended device was equipped with CO₂ laser.

TABLE 2

Conditions of laser micro-treatment testing of the silicon solar cells electrodes made from paste A

Series	Solar cell surface	Thickness of front electrode, μm	Laser beam feed rate (v), mm/s	Laser beam (P), W
1	1,2,3,4	15, 35	37.8, 40.5, 43.2	50
2	1,2,3,4	15, 35	48.5, 51.3, 54	100
3	1,2,3,4	60	21.6 24.3 27	50

Where: 1. non-textured with deposited TiO_x coating, 2. non-textured without deposited TiO_x coating, 3. textured with deposited TiO_x coating, 4. textured without deposited TiO_x coating

TABLE 3

Conditions of co-firing process of the silicon solar cells testing electrodes (the thickness of front electrode: 15, 40, 60 μm)

Series	Paste symbol	Temperature, °C		
		Zone I	Zone II	Zone III
1	C, D, E, F	530	570	830
				860
				890
				920
				945
2	PV 145	530	570	830
				860
				890
				920

In a case of co-firing in the conveyor belt IR furnace were prepared some solar cells with the test electrodes system I, II (Tab. 3). The belt IR furnace was equipped with fitted tungsten filament lamps, heating both the top and bottom of the belt (the belt feed rate was 200 cm/min).

The kind of the problem was determined as the standard, in which every vector is independent from another vector. The

assignment of vectors to training, validation or testing set was random. The search for the optimal network was restricted to architectures such as [18,19,20,24,25]:

- radial basis function network (RBF), 1
- linear networks,
- generalized regression neural network (GRNN),
- multi-layer perceptron (MLP).

Input values were :

- paste symbol,
- sample symbol,
- surface morphology of the solar cell,
- number of test electrode system,
- current [10, 30 and 50 mA],
- thickness of screen printed front electrode,
- co-fired temperature (convectional method),
- laser beam feed rate and laser beam (unconventional method).

3. Methodology

The investigations of contact resistance R_c , of front contact solar cell using the Transmission Line Model (TLM) method onto measuring position was determined in the Institute of Engineering Materials and Biomaterials. TLM consists in direct current (I) measurement and voltage (U) measurement between any two separate contacts.

The set of all descriptive vectors were divided into three subsets in the relation 2-1-1. The first set contains the half of all vectors and was used for the modification of the neuron weights (training set). One fourth of the vectors were used for valuation of prediction errors by training process (validation set). Remaining vectors were used for the independent determination of prediction correctness, when the training process is finished. Networks were trained with use of the back propagation and conjugate gradient methods. [20,22,23]. For verification of networks usability for the aims of parameters prediction the following parameters of the quality valuation were used:

- average absolute error – difference between measured and predicted output values of the output variable,
- standard deviation ratio – a measure of the dispersion of the numbers from their expected (mean) value. It is the most common measure of statistical dispersion, measuring how widely the values in a data set are spread,
- Pearson correlation – the standard Pearson-R correlation coefficient between measured and predicted output values of the output variable.

All computations were made by the use of Statistica Neural Network by Statsoft, the most technologically advanced and best performing neural networks application on the market. It offers numerous selections of network types and training algorithms and is useful not only for neural network experts [27].

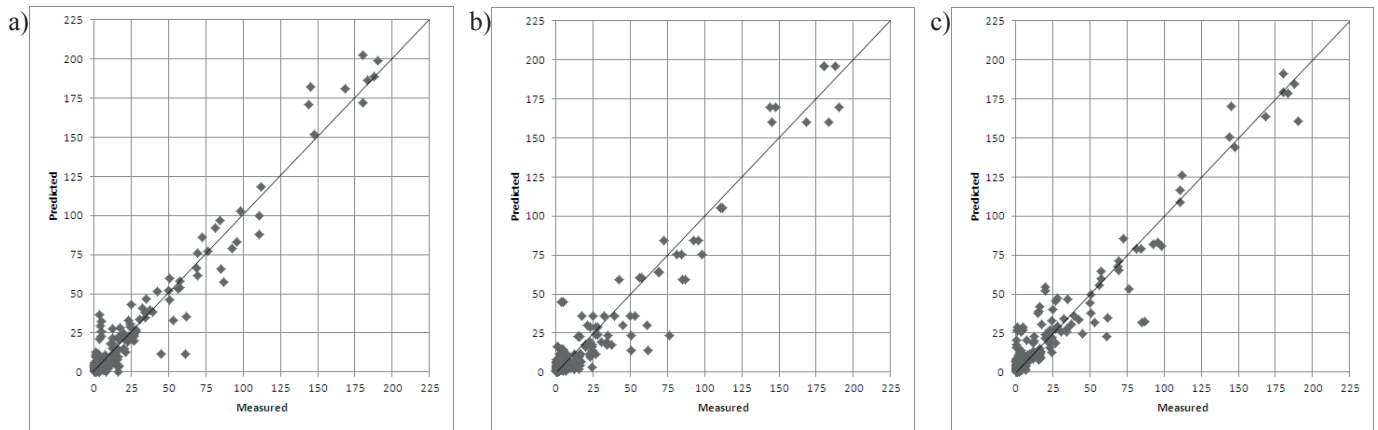


Fig. 3. Comparative graph of measured and predicted values of contact resistance of solar cells obtained by method 1: a) training set, b) validation set, c) testing set

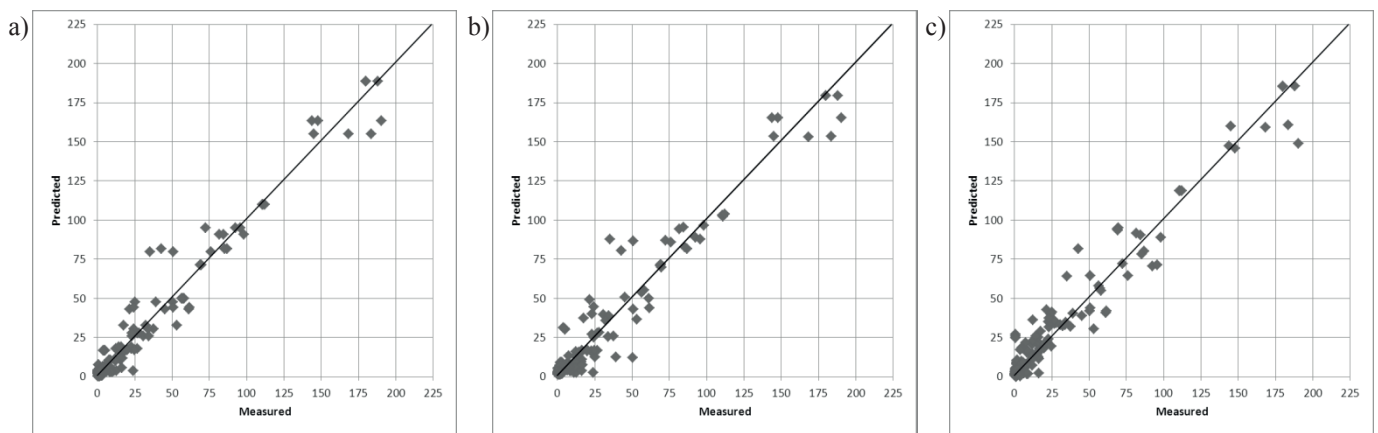


Fig. 4. Comparative graph of measured and predicted values of contact resistance of solar cells obtained by method 2: a) training set, b) validation set, c) testing set

4. Modeling results

The best results were obtained for the multi-layer perceptron architecture with two hidden layers (Fig.2). Type of this network for individual properties along with the numbers of used neurons and the quality valuation parameters for all three sets are introduced in the Table 4.

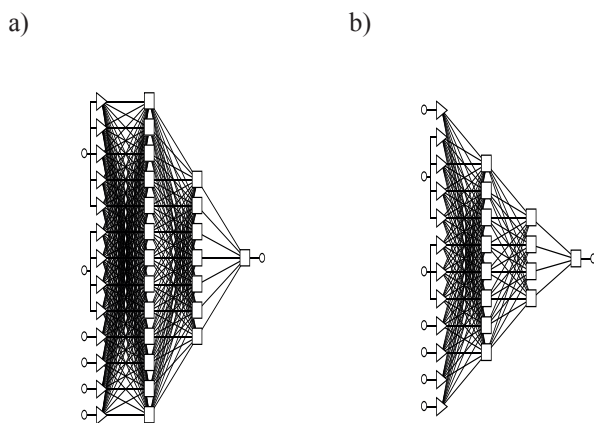


Fig. 2. Architectures of neural net used to predict the contact resistance, a) method 1, four-layer perceptron 6:13-13-7-1:1, b) method 2, four-layer perceptron 7:12-8-4-1:1

For all trained networks the Pearson correlation coefficient has reached the value above 90 % and comparatively low values of the standard deviation ratio. This is very good representation of estimated properties. For every estimated parameter the vectors distribution is comparable for all three subsets. This indicates the correctness of the prediction process. Significant differences in vectors distribution among groups would mark the possibility of excessive matching to training vectors, and the bad quality of the network.

Correlation charts between measured and predicted values of solar cells contact resistance for training, validation and testing sets are presented in figure 3 for method 1 and in figure 4 for method 2.

After the development of artificial neural networks a sensitivity analysis was performed to estimate how big is the influence factor of production conditions on silicon solar cells contact resistance. It was found, that in case of method 1 the biggest influence has co-fired temperature and the smallest – current. In case of method 2 the biggest influence on contact resistance value has laser beam feed rate, the smallest – current. Detailed results are shown in table 5 for method 1 and in table 6 for method 2. Quotients of all production conditions from both methods of production exceeded the threshold limit set at 1.05, which means that their impact on contact resistance is significant.

TABLE 4

Parameters of computed artificial neural networks used to predict the contact resistance

Met-hod	Net -work type	Network archite- cture	Training set			Validation set			Testing Set		
			AAE	SDR	PC	AAE	SDR	PC	AAE	SDR	PC
1	MLP 4	6:13-13-7-1:1	1.02	0.23	0.971	1.45	0.28	0.961	1.17	0.23	0.973
2	MLP 4	7:12-8-4-1:1	0.01	0.24	0.972	0.05	0.27	0.961	0.06	0.30	0.971

AAE – average absolute error, SDR – standard deviation ratio, PC - Pearson correlation

TABLE 5

Sensitivity analysis of production conditions of solar cells on contact resistance obtained by method 1

	Range	Error	Quotient
co-fired temperature	1	30.89	4.36
paste symbol	2	20.77	2.93
surface morphology of the solar cell	3	20.66	2.91
number of test electrode system	4	16.36	2.31
thickness of screen printed front electrode	5	10.05	1.41
current	6	7.89	1.11

TABLE 6

Sensitivity analysis of production conditions of solar cells on contact resistance obtained by method 2

	Range	Error	Quotient
laser beam feed rate	1	3.68	11.86
paste symbol	2	1.49	4.81
thickness of screen printed front electrode	3	1.38	4.45
surface morphology of the solar cell	4	1.34	4.33
laser beam	5	1.28	4.14
number of test electrode system	6	0.40	1.30
current	7	0.34	1.12

5. Conclusions

Results obtained from the given ranges of input data show very good ability of artificial neural networks to predict the contact resistance of the silver electrode-silicon junction. The Pearson correlation coefficient over 90 % and low deviation ratio inform about the correct execution of the training process. The uniform distribution of vectors in every set indicates good ability of the networks to results generalization.

Obtained results have confirmed the correctness of the artificial neural networks usage as the simulating tool. It makes possible to apply this networks in the area of material engineering for the prediction of the contact resistance of manufactured front metallization.

The results of new research will be supporting and complementing the research undertaken in the present project. In effect they can develop the existing knowledge and experience in this paper.

Acknowledgements

The authors thank Prof. L. A. Dobrzański for valuable directions during implementation of this work.

REFERENCES

- [1] L.A. Dobrzański, M. Muszytyfaga, A. Drygała, Final manufacturing process of front side metallisation on silicon solar cells using convectional and unconventional techniques, *Strojnicki Vestnik - Journal of Mechanical Engineering* 59 3, 175-182 (2013).
- [2] M. Muszytyfaga, L. A. Dobrzański, S. Ruz, L. Prokop, S. Misak, Application of modern technique to set the paramaters of the monocrystalline solar cell and its structure, *Electrotechnical Review*, ISSN 0033-2097, R. 89 NR 11, p. 24-26 (2013).
- [3] L.A. Dobrzański, M. Muszytyfaga, A. Drygała, P. Panek, Investigation of the screen printed contacts of silicon solar cells from Transmissions Line Model, *Journal of Achievements in Materials and Manufacturing Engineering, JAMME*, 41 1-2, 57-65 (2010).
- [4] L.A. Dobrzański, M. Muszytyfaga, Effect of the front electrode metallisation process on electrical parameters of a silicon solar cell, *Journal of Achievements in Materials and Manufacturing Engineering*, 48 /2, 2011, Issue 2, 115-144 (2011).
- [5] L.A. Dobrzański, M. Muszytyfaga, A. Drygała, W. Kwaśny, P. Panek, Structure and electrical properties of screen printed contacts on silicon solar cells, *Journal of Achievements in Materials and Manufacturing Engineering, JAMME*, 45 2, 141-147 (2011).
- [6] F. Clement, M. Menkoe, R. Hoenig, J. Haunschild, D. Biro, R. Preu, D. Lahmer, J. Lossen, H.J. Krokoszinski, Pilot-line processing of screen-printed Cz-Si MWT solar cells exceeding 17 % efficiency, *Proceedings of Photovoltaic Specialists Conference (PVSC)*, 34th IEEE, 223-227 (2009).
- [7] M. Burgelman, Thin film solar cells by screen printing technology. *Proceedings of The Workshop Micro technology and Thermal Problems in Electronics*, 129-135 (1998).
- [7] J.P. Boyeaux, H. El. Omari, D. Sarti, A. Laugier, Towards an improvement of screen printed contacts in multicrystalline

- silicon solar cells, Proceedings of 11th European Photovoltaic Solar Energy Conference and Exhibition, 12-16 October, 1-4 (1992).
- [7] L. Gautero, M. Hofmann, J. Rentsch, A. Lemke, S. Mack, J. Seiffe, J. Nekarda, D. Biro, A. Wolf, B. Bitnar, J.M. Sallese, R. Preu, All-screen-printed 120- μm -thin large-area silicon solar cells applying dielectric rear passivation and laser-fired contacts reaching 18% efficiency, Proceedings of Photovoltaic Specialists Conference (PVSC), 34th IEEE, 1888-1893 (2009).
- [8] P. Hacke, J.M. Gee, A screen-printed interdigitated back contact cells using a boron-source diffusion barrier, Solar Energy Materials and Solar Cells 88, p. 119-127(2005).
- [9] M.M. Hilali, B. To, A. Rohatgi, A review and understanding of screen-printed contacts and selective-emitter formation, Conference paper – Workshop on crystalline silicon solar cells and modules, Winter Park, Colorado, 1-8 (2004).
- [10] A. Mette, C. Schetter, D. Wissen, S.W. Glunz, G. Willeke, Increasing the efficiency of screen-printed silicon solar cells by light-induced silver plating, Proceedings of the 4th World Conference on Photovoltaic Energy Conversion, Waikoloa, Hawaii, USA, 1056 (2006).
- [11] M. Mohamend, J.M. Gee, P. Hacke, Bow in screen-printed back contact industrial silicon solar cells, Elsevier, Solar Energy and Solar cells 91(13), 1128-1233 (2007).
- [12] W. Neu, A. Kress, W. Jooss, P. Fath, E. Bucher, Low-cost multicrystalline back-contact silicon solar cells with screen printed metallization, Solar Energy Materials and Solar Cells 74(1-4), 139-146 (2002).
- [13] H.El. Omari, J.P. Boyeaux, A. Laugier, Screen printed contacts formation by rapid thermal annealing in multicrystalline silicon solar cells, Proceedings of 25th PVSC, Washington, 585-588 (1996).
- [14] H. Exner, P. Regnefuss, L. Hartwig, S. Klötzer, R. Ebert, Selective laser sintering with a Novel Process, Proceedings of 4th International Symposium on Laser Precision Microfabrication, Munich, 145-151 (2003).
- [15] M. Alemán, A. Streek, P. Regenfuß, A. Mette, R. Ebert, H. Exner, S.W. Glunz, G. Willeke, Laser micro-sintering as a new metallization technique for silicon solar cells. Proceedings of the 21st European Photovoltaic Solar Energy Conference, Dresden, Germany, 705 (2006).
- [16] L.A. Dobrzański, R. Honysz, Artificial intelligence and virtual environment application for materials design methodology, Journal of Machine Engineering 11/1-2, 102-119 (2011).
- [17] Markowska-Kaczmar U. (ed.), Neural networks in applications, Wrocław University of Technology publishing office, Wrocław, 1996, (in Polish).
- [18] T. Masters, Neural networks in practice, PWN, Warsaw.
- [19] W.S. McCulloch, A logical calculus of the ideas immanent in nervous activity, Bulletin of Mathematical Biophysics 5, 115-133(1943).
- [20] D. Rutkowska, M. Pilinski, L. Rutkowski, Neural networks, genetic algorithms and fuzzy systems, PWN, Warsaw, 1996, (in Polish).
- [21] R. Tadeusiewicz, Elementary introduction for neural networks techniques with sample applications, Academic Publishing House PLJ, Warsaw, 1998, (in Polish).
- [22] L.A. Dobrzański, R. Honysz, Application of artificial neural networks in modelling of normalised structural steels mechanical properties, Journal of Achievements in Materials and Manufacturing Engineering 32/1 37-45 (2009).
- [23] L.A. Dobrzański, R. Honysz, Application of artificial neural networks in modelling of quenched and tempered structural steels mechanical properties, Journal of Achievements in Materials and Manufacturing Engineering 40/1 50-57(2010).
- [24] J. Żurada, M. Barski, W. Jedruch, Artificial neural networks. PWN, Warsaw, 1996, (in Polish).
- [25] <http://www.statsoft.pl/>

Received: 10 October 2014.